Thermal Analysis of Micromirrors for High-Energy Applications

Jianglong Zhang, Yung-Cheng Lee, Adisorn Tuantranont, and Victor M. Bright, *Member, IEEE*

***Abstract*—This paper presents the results of an investigation of thermal mechanism between laser and surface-micromachined micromirrors. Finite element models by use of ABAQUS are established and used to study the temperature distribution on the surface of micromirrors under the high-power laser illumination. It is shown that the heat conduction through the gas gap between the mirror surface and the substrate is the dominant thermal dissipation mechanism for the high surrounding gas pressure, while the heat conduction through the flexures is dominant for the low surrounding gas pressure. Based on the simulation results, two novel methods are proposed in order to tolerate more power input under a low surrounding gas pressure. The results of optical power testing validate these models, and indicate that these two approaches are efficient in improving micromirror performance for high-energy applications.**

***Index Terms*—Finite element, microelectromechanical systems (MEMS), micromirror, thermal analysis.**

I. Introduction

Surface-micromachined micromirrors have received considerable attentions for the development of optical systems. Many applications of microelectromechanical systems (MEMS) require optical power levels that are large in comparison to the size of the micro-optical structures [1]–[3]. For example, micromirror arrays are subjected to high heat fluxes from an external light source when it is used for laser modulation. The reliability and performance of the mirrors are related to their operating temperature [4]. High temperature can distort reflective surfaces, reduce the optical efficiency of the system or even ablate micromirror surfaces and melt supporting flexures [5], [6]. Therefore, thermal management is a key consideration in the design of micromirror devices and their packages. However, since the study of micromirrors for high-energy applications is still in progress as of this time, methods to improve the heat transfer performance of micromirrors are limited. In 1998, David and Bright investigated optical power induced damage to MEMS-based micromirrors [5]. A mathematical model was developed and used to predict the minimum incident optical power that will permanently damage the reflective surface of a micromirror. One typical micromirror they studied is shown in Fig. 1 (Design 1). In fact, the mathematical model they established was based on the assumption that the temperature on the surface of a micromirror was uniform, which was not accurate for the high surrounding gas pressure [7]. More accurate models are required to study the thermal mechanism between laser and micromirrors. Moreover, optical power testing indicated that the lowest observed optical power resulting in damage was 7.5 mW for this design under a low surrounding gas pressure (0.02 Torr). This power is not big enough for micromirrors in many high-energy applications. New designs of micromirrors to tolerate more power input are also needed. It is also very important to know the thermal mechanism between lasers and mirrors under different conditions to find more reliable designs of devices and packages.

In this paper, three-dimensional (3-D) finite element models are established and used to study different effects on the temperature distribution on the surface of micromirrors. The effects studied are surrounding gas pressure in the micromirrors package, the gold surface reflectivity, and the geometry of micromirrors. Micromirrors are usually hermetically sealed in chip carriers to prevent dust and moisture contamination. Low pressure package is desirable in order to obtain high speed modulation. Based on simulation results, two novel methods are proposed in order to tolerate more power input for low pressure surrounding gas. It turns out that the results of optical power testing are consistent with these models, and demonstrates the efficiency of these two approaches in terms of improving micromirror performance for high-energy applications.

II. Micromirror Configuration and Finite Element Model

Micromirrors studied in this paper were fabricated through the production run of the multi-user MEMS processes (MUMP's) from Cronos Integrated Microsystems [8]. MUMP's offer three patternable layers of polysilicon, and two sacrificial layers of phosphosilicate glass on a base layer of silicon nitride. A top layer of gold is used as the reflective surface. After fabrication, MEMS devices are "released" by removing sacrificial glass layers in buffered hydrofluoric acid (HF). Fig. 2 depicts the micromirror's structure after release studied in this paper (Design 2). It consists of a top electrode formed out of Poly1, Ploy2, trapped oxide and gold suspended 2.0 μm above one-bottom Poly0 electrodes. Dimples are put at the end of flexures to protect the mirror from the electrostatic snap-through effect. The micromirror is driven by an electrostatic force. If a voltage is applied between the top electrode

Manuscript received July 12, 2001; revised July 8, 2003. This work was supported by the Air Force Office of Scientific Research (AFOSR), Bolling AFB, Washington, DC, under Grant F49620-98-1-0291.

J. Zhang is with the Reflectivity, Inc., Sunnyvale, CA 94085 USA (e-mail: jianglong@reflectivity.com).

Y.-C. Lee and V. M. Bright are with Department of Mechanical Engineering, University of Colorado, Boulder, CO 80309-0427 USA.

A. Tuantranont is with the National Electronics and Computer Technology Center, Klongluang, Pathumtani 12120, Thailand.

Digital Object Identifier 10.1109/TADVP.2003.818050

1521-3323/03$17.00 © 2003 IEEE

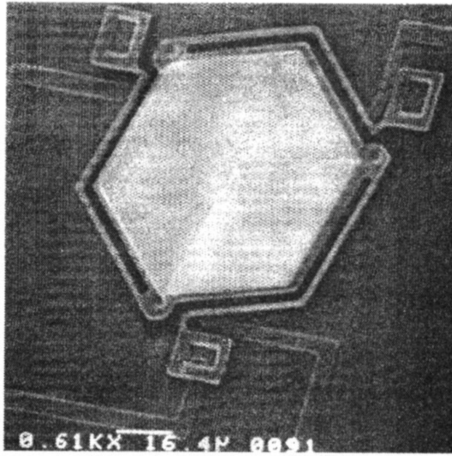

Fig. 1. Surface-micromachined electrostatically-actuated micromirror studied in [5], [6] (design 1).

and bottom electrode, it will be pistoned down, lengthening the optical path of light reflected off the micromirror. Pistoning is used for phase modulation in coherent systems.

All modeling and optical power testing in this paper is based on the assumption that the micromirror is at steady state. When a micromirror is at steady state, the thermal power absorbed from a laser is equal to the thermal power dissipated. There are three heat transfer paths that can remove the thermal power from a micromirror, which are surface radiation, heat conduction through flexures to silicon substrate and heat conduction through surrounding gas to silicon substrate. Micromirrors are usually hermetically sealed in chip carriers to prevent dust and moisture contamination: external forced gas convection is usually not practical. Because of the small scale of the micromirror, free convection can be neglected [9]. Fig. 3 shows the diagram of heat transfer paths and boundary conditions used for simulations [10].

If only the gold region of the micromirror in Fig. 1 is illuminated, the absorbed optical power is proportional to the incident power, P. Equation (1) calculates the absorbed power, P_a

$$P_a = \lfloor 1 - R_g(\lambda) \rfloor \cdot P \tag{1}$$

$R_g(\lambda)$ is the reflectivity of gold. It is a function of the wavelength of the source, λ. All unreflected power is absorbed by the gold and underlying polysilicon layers.

Thermal power dissipated by surface radiation, $Q_{r.}$, is given by (2)

$$Q_r = \varepsilon\sigma \left(T^4 - T_s^4\right) \cdot A_r \tag{2}$$

ε is the emissivity, σ is Boltzmann's constant, T_s is the surrounding temperature and A_r is the surface area. Thermal conduction through gas gap to the silicon substrate depends on both the composition and pressure of the gas. Equation (3) calculates the thermal power dissipated by the top electrode through the gas gap to the bottom electrodes and substrate, $Q_{g,con}$

$$Q_{g,con} = A_{g,con} \cdot \frac{k_g p}{p_0} \cdot \frac{\Delta T}{d} \tag{3}$$

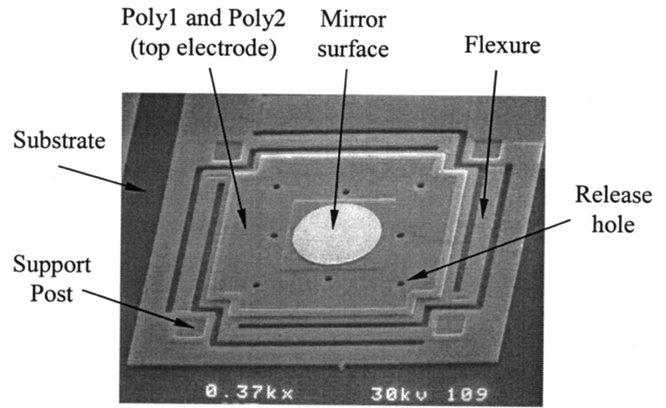

Fig. 2. Surface-micromachined electrostatically-actuated micromirror studied in this paper (design 2).

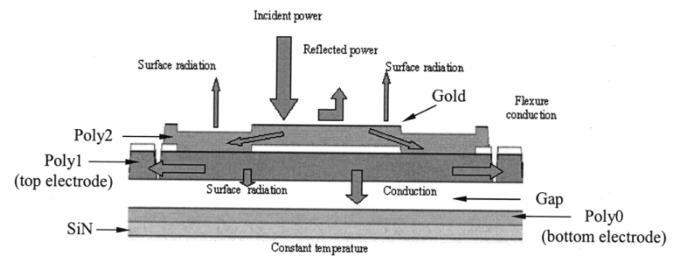

Fig. 3. Diagram of heat transfer paths (cross section view).

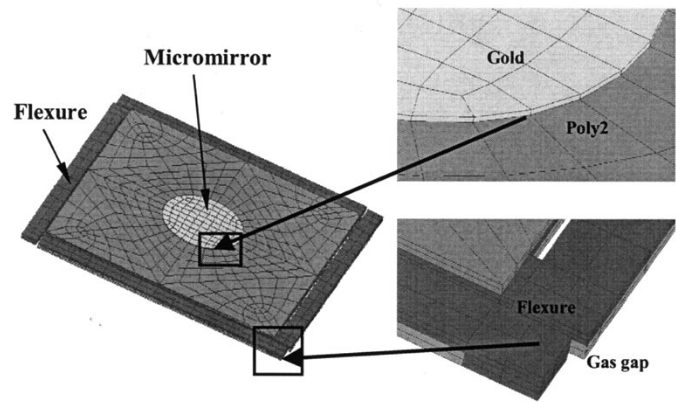

Fig. 4. Finite element model.

here k_g is the thermal conductivity of the surrounding gas at a reference pressure p_0, p is the pressure of the surrounding gas, ΔT is the temperature difference along the direction of heat dissipation and d is the separation distance between the top and bottom electrodes, $A_{g,con}$ is the conduction area of the surrounding gas between the top and bottom electrodes. Thermal conduction of the top and sides of the top electrode through the surrounding gas to the micromirror package also dissipates energy; however, the separation distance between the top and bottom electrodes (2.0 $\mu\mathrm{m}$ for micromirror in Fig. 2) is much less than the distance between the top electrode and the micromirror package (typically >1 mm for micro-optical device packaging). Thermal conduction through the surrounding gas to the micromirror package is more than two orders of magnitude less than the value predicted by (3), so it can be neglected with

TABLE I
VARIABLES AND MATERIAL PROPERTIES FOR THE SIMULATION

Boltzmann constant (σ), W/m^2K^4 [10]	5.67E-8
Maximum allowable device temperature (T_d), K	523
Temperature of substrate and surrounding environment (T_s), K	295
Measured reflectance of gold (R_g), % [5,6]	91.5
Estimated emissivity of polysilicon (ε_p), % [9]	20
Emissivity of gold (ε_g), % [10]	3
Thermal conductivity of phosphorous-doped polysilicon (K_p), W/mK [11]	29
Thermal conductivity of air at 295K(K_g), W/mK [12]	0.0252
Pressure in test chamber (ρ), Torr	0.001
Reference pressure (ρ_0), Torr (1 atm)	760

TABLE II
OPTICAL POWER RATING DISSIPATED THROUGH DIFFERENT THERMAL PATHS FOR HIGH GAS PRESSURE (ABSORBED POWER: 85 mW, MAXIMUM SURFACE TEMPERATURE FROM SIMULATION: 606 K, SURROUNDING GAS PRESSURE: 760 TORR)

Thermal Path	Gold Radiation	Poly2 radiation	Poly1 radiation	Gas gap conduction	Flexure conduction
Power rating (mW)	0.00558	0.0141	0.0158	80.7645	4.2
Percentage	0.0047	0.0167	0.0186	95.02	4.94

TABLE III
OPTICAL POWER RATING DISSIPATED THROUGH DIFFERENT THERMAL PATHS FOR LOW GAS PRESSURE (ABSORBED POWER:4.25 mW, MAXIMUM SURFACE TEMPERATURE FROM SIMULATION: 640 K, SURROUNDING GAS PRESSURE: 0.02 TORR)

Thermal Path	Gold Radiation	Poly2 radiation	Poly1 radiation	Gas gap conduction	Flexure conduction
Power rating (mW)	0.00765	0.0385	0.04	0.0289	4.135
Percentage	0.183	0.906	0.941	0.68	97.29

only a minimal impact on the model's accuracy. Thermal conduction through flexures to the silicon substrate is dependent on the geometry of flexures. Equation (4) calculates the thermal power dissipated by flexures to the substrate, $Q_{f,con}$

$$Q_{f,con} = A_{f,con} \cdot k_p \cdot \frac{\Delta T}{L} \tag{4}$$

where k_p is the thermal conductivity of the polysilicon, L is the length of the flexures and $A_{f,con}$ is the conduction areas of the flexures.

When a micromirror is in thermal equilibrium, the thermal power absorbed is equal to the thermal power dissipated, as shown in (5)

$$P_a = Q_r + Q_{f,con} + Q_{g,con}. \tag{5}$$

In order to compute the temperature distribution of the micromirror when it is under direct laser illumination, a 3-D finite element model (FEM) with the use of ABAQUS is established. Fig. 4 illustrates the model. In this model, it is assumed that only the gold region of the micromirror is illuminated. The laser

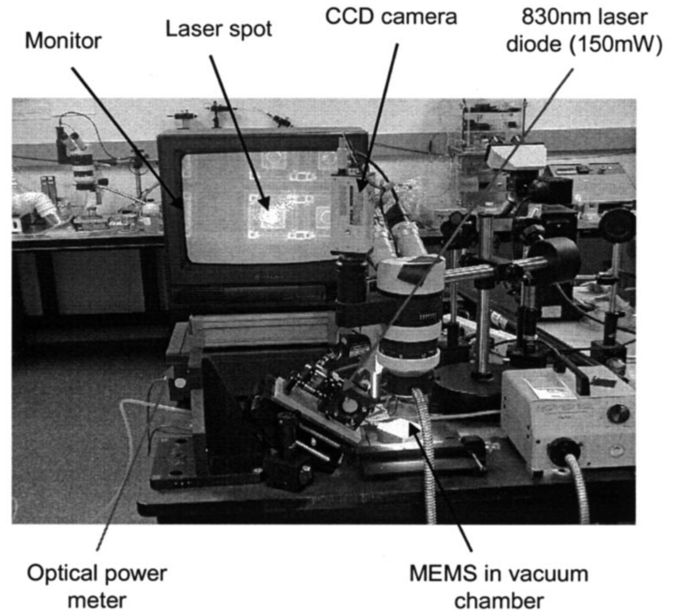

Fig. 5. Optical power testing set-up.

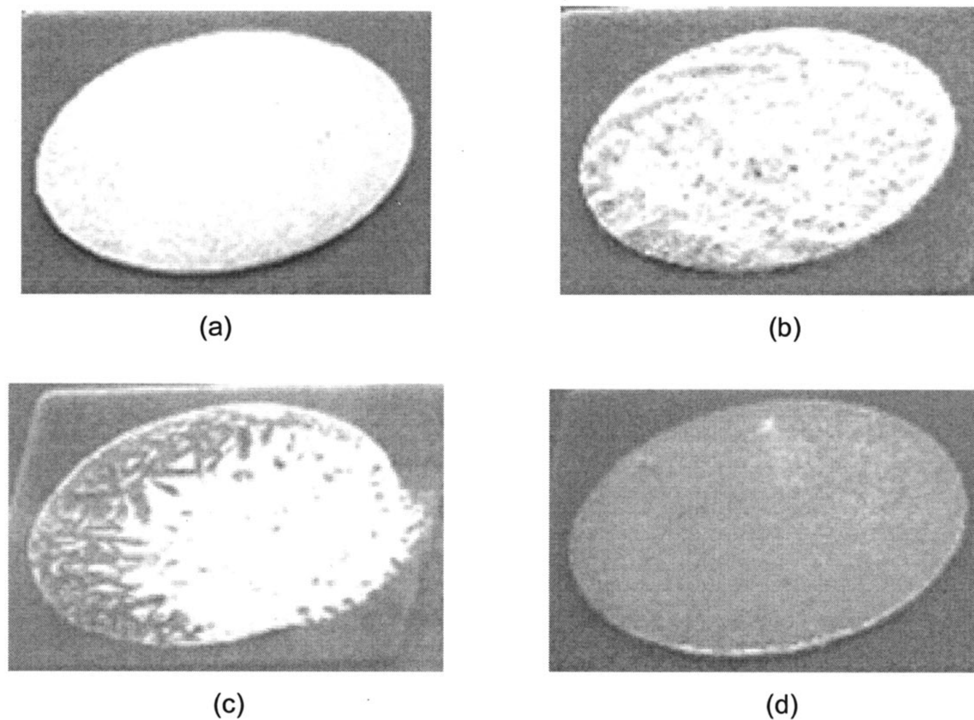

Fig. 6. Surface change for different incident power: (a) original mirror surface (after release), (b) reaction begins (incident power: 58.5 mW), (c) reaction expands (incident power: 65 mW), and (d) gold reacts with polysilicon completely (incident power: 80 mW).

power is modeled as heat flux through top gold surface from outside. The input power is the "absorbed power," as defined by (1). Different thermal conductivity is assigned to the air gap for different surrounding gas pressure, shown in (3). Actually, (3) is for macroscopic gas conduction in air. It might not be true for high temperature and low surround gas pressure. These effects are neglected in this paper. Since the contact area of support posts is much larger than the cross section area of the flexures, their thermal resistance is much smaller than the thermal resistance of the flexure. Therefore, the support posts are not included in the FEM model. Under direct illumination, the highest temperature in the micromirror is the temperature at the center of the gold layer. When this temperature exceeds a threshold value, the micromirror will suffer a permanent damage. Variables and material properties for simulation are shown in Table I. Once the temperature distribution is obtained, thermal power dissipation through different path can be calculated by integrating the heat flux at the specified area based on (2)–(4).

III. Simulation Results

In order to identify the thermal mechanism under different conditions, several parameters are studied in this paper. These parameters are the gold surface reflectivity, the gas pressure in micro-mirrors package, and the device's geometry.

Gold surface reflectivity is an important factor considered. If the reflectivity decreased from 91.5% to 61.5%, the maximum temperature on the micro-mirror would increase from 98 °C to 303 °C when the incident power is 9.347 mw and the surrounding nitrogen gas pressure is 0.02 Torr. It can be even worse that the surface reflectivity is reduced when the temperature increases. The reflectivity effect was identified as a major factor to cause the micro-mirror structural damage in a short period of time.

Gas pressure is another important factor. Tables II and III show the power dissipated through different thermal paths for different surrounding gap pressures. The gas gap conduction dissipates more than 95% absorbed thermal energy when the gas pressure is equal to 760 Torr (Table II). Therefore, thermal conduction through surrounding gas to the substrate is the dominant thermal energy mechanism for gas pressures at or above 760 Torr. But if the pressure of the surrounding gas is very low (0.02 Torr), then the dominant thermal energy dissipation mechanism is thermal conduction through flexures. Table III illustrates that flexure conduction dissipates more than 97% absorbed thermal energy under this condition. Surface radiation can be neglected for both conditions if the maximum surface temperature is less than 500 °C.

Since the dominant thermal dissipation mechanism is different for different gas pressures, different methods to reduce the surface temperature of the micromirror should be proposed. For high gas pressure, gas gap conduction is the critical thermal path. Using gas with high thermal conductivity (for example: helium) can reduce the surface temperature apparently. Micromirrors are usually hermetically sealed in chip carriers to prevent dust and moisture contamination. Low pressure package is desirable in order to obtain high speed modulation. The dominant thermal energy dissipation mechanism is thermal conduction through flexures to the silicon substrate if the pressure of the surrounding gas is very low. Flexure design is the main factor of consideration in order to reduce the surface

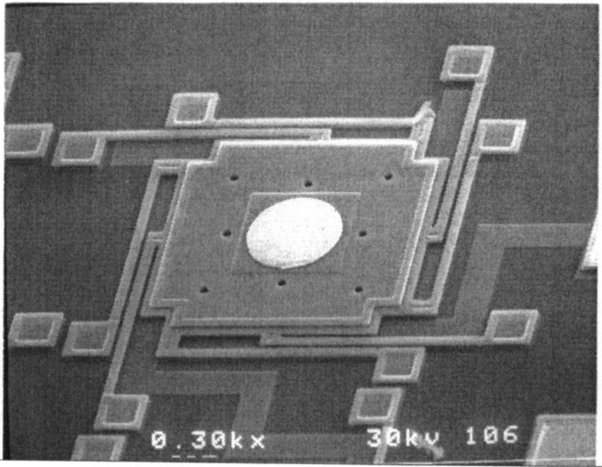

Fig. 7. Improved design: two flexures along each side (design 3).

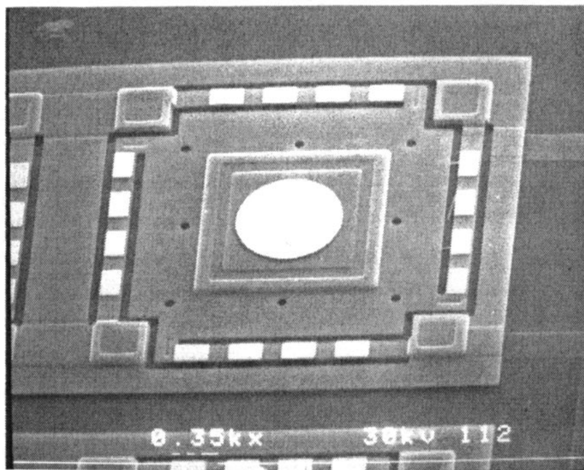

Fig. 8. Improved design: gold on flexures (design 4).

temperature under this condition. The following optical power testing and simulation is for low surrounding gas pressure.

IV. Optical Power Testing

Previous thermal testing demonstrates that micromirrors baked at temperatures of 250 °C or higher causes visible damage to the gold reflective region [5], [6]. The thermal damage visually appears as a discoloration and a loss of planarity (appearance of small bumps) in the gold layer. Polysilicon and silicon nitride layers suffer no visible damage. So 250 °C is chosen as a device failure threshold temperature. When the maximum surface temperature reaches this value, the amount of incident optical power is defined as the minimum optical power that will damage the micromirror for the simulation. A power at 150 mW supplied by a power-adjustable continuous wave laser diode is used as the incident optical power. Fig. 5 is the picture of the optical power testing set-up. The MEMS device is put in the vacuum chamber with a glass cover. A molecular pump connects the chamber with a hard plastic pipe. When the pump is on, the air in the chamber is drawn away until the pump reaches its steady state (0.001 Torr). The laser's output is focused by the focusing lens in the laser diode device so that the laser's spot filled the gold reflective surface but did not fall on the polysilicon border. A microscope with CCD camera is located above the chamber and used to grab pictures of the device. These pictures can be shown on a color monitor and used to check the size and location of the laser spot. The optical power is measured by an optical power meter. A new micromirror is used for each test. Losses in the glass cover of the vacuum chamber reduce the optical power incident on the micromirror to 90% of the optical power exiting the focusing lens in the laser diode device. The test device is put on a large copper stage in the chamber during the experiment. The vacuum chamber is also made of copper. Therefore, the heat from the mirror surface can be dissipated very quickly through the stage and the chamber

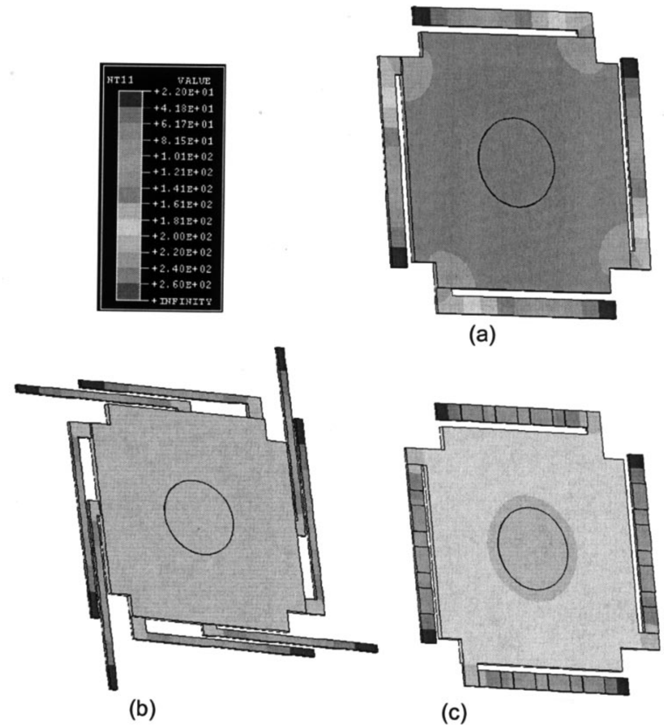

Fig. 9. Surface temperature distribution for different micromirrors. (Incident power: 52.3 mW, the maximum surface temperature: (a) 250 °C, (b) 178 °C, and (c) 210 °C).

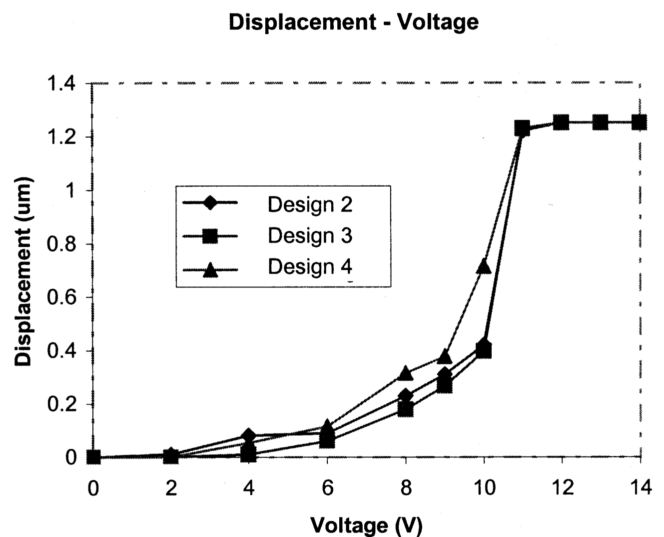

Fig. 10. Electrical-mechanical test for different micromirrors.

TABLE IV
MEASUREMENT RESULTS OF OPTICAL POWER RATING

Different designs	Threshold power(mW) (experiment)	Threshold power(mW) (simulation)
Old design (poly 1, one flexure, without gold)	58.5	52.3
Old design (poly 2, one flexure, without gold)	45.6	40.8
Improved Design (Poly 2, one flexure, with gold)	72.5	66.2
Improved Design (Poly 1, two flexures, without gold)	91	80.7
Improved Design (Poly 2, two flexures, without gold)	72.6	64.3
Improved Design (Poly 2, two flexures, with gold)	109.1	98.7

to hold the substrate at the surrounding room temperature (22 °C) during the test.

Fig. 6 shows the surface change for different incident power. After release, the original micromirror surface is very flat and the reflectivity is more than 90% (Fig. 6(a)) [11]. Surface change could not be observed until the incident power is equal or larger than a threshold value 250 °C [5]. At this threshold value, the gold surface becomes rough and surface reflectivity falls to less than 50% [Fig. 6(b)]. Bright surface becomes dark in a very short time (less than half a minute). This threshold value is defined as the minimum optical power resulting in damage for the micromirrors obtained by optical power testing. The thermal damage is likely due to a widening of the eutectic bond under the gold layer, release of the phosphorous (which boils at 280 °C) in the polysilicon under the gold, or a combination of these effects [5]. As the power rises, the gold layer reacts with the polysilicon layer and partly becomes to another material [Fig. 6(c)]. If the incident power is large enough, the gold layer will completely disappear [Fig. 6(d)]. The mechanism of this reaction needs to be further investigated [12].

V. DISSCUSSION

Using a device failure threshold temperature of 250 °C, the simulation results show that the amount of optical power required to damage the reflective layer is 52.3 mW for the micromirror of Design 2. It is 7-time larger than the optical power causing damage to the micromirror of Design 1. One reason for this difference is that there are 4 flexures for the micromirror shown in Design 2 instead of 3 flexures for the micromirror shown in Design 1. More flexures can reduce the thermal resistance of micromirrors and then dissipate more thermal energy. Flexure width is another reason for better energy dissipation. The width of flexures is 2.0 μm in Design 1, whereas 12.0 μm in Design 2. Wide flexures also reduce the thermal resistance of micromirrors and cause the increment of minimum optical power induced damage to micromirrors. The threshold power is 58.5 mW obtained from optical power testing, which gets good agreements with simulation results.

Although 7-time increment of minimum optical power has been obtained for the micromirror of Design 2, its electrical-mechanical performance is changed. Increasing the flexure width or the number of flexures could decrease the surface temperature but would increase the stiffness of flexures and then the applied voltage in order to get the same displacement. These methods are not good. Good methods should lower the surface temperature without affecting the electrical-mechanical performance of micromirrors. One method to lower the surface temperature is to use two flexures instead of one flexure along each side to reduce the thermal resistance of the micromirror. This new design is shown in Fig. 7 (Design 3). The length of flexures is the same as that of Design 2 and the width of flexures is half of that of Design 2. Thus the total stiffness of flexures is almost the same for both designs, and then the electrical-mechanical performance will not be affected for this improved design. Coating gold on flexures (Fig. 8, Design 4) is another desirable method to reduce the thermal resistance of flexures because the thermal conductivity of gold is much larger than that of polysilicon. Segmented gold slices are chosen to avoid warpage of flexures induced by the CTE difference between gold and polysilicon. The Young's Modulus of gold (80 GPa) [13] is much smaller than the Young's Modulus of polysilicon (169 GPa). The coating thickness of gold for MUMP's (0.5 μm) is also much smaller than the thickness of poly 2 (1.5 μm). Therefore, effects of gold layer on stiffness of flexures can be neglected. The electrical-mechanical performance of this design is almost the same as Design 2.

Fig. 9 shows the simulation results of the surface temperature distribution for different micromirrors when the incident optical power is 52.3 mW. Different colors represent different temperatures. The maximum surface temperature will fall from 250 °C to 210 °C if there is a gold layer on flexures and will fall from 250 °C to 178 °C if there are two flexures along each side instead of one flexure. The results indicate that these two approaches are efficient ways to increase micromirror performance for high-energy applications.

Fig. 10 presents the experiment results of electrical-mechanical performance for different micromirrors. These two improved micromirrors almost have the same pull-in voltage with the micromirror of Design 2. These results indicate that those two proposed methods for better heat transfer do not affect their electrical-mechanical performance.

The threshold optical power for all kinds of micromirrors obtained from simulation and optical power testing is listed in Table IV. The lowest observed optical power resulting in damage is about 10% higher than the simulation results in all cases. Variations between the simulated and observed values may be due to the estimate of the emissivity of the polysilicon. Published emissivity measurements of MUMP's polysilicon are not found. Variations may also result from an inaccurate estimate for the thermal conductivity of the polysilicon. The thermal conductivity of the polysilicon used in MUMP's may be higher than the value listed in Table I. Spot size of the laser beam may be another factor, which causes the variations. The actual spot size of the laser beam may be larger than the gold layer. The actual width of the support flexures varies slightly from design values, depending on fabrication etch rates and times. The sides of top electrodes and the top of flexures also dissipate thermal power to the surrounding gas.

Table IV also indicates that the two approaches previously proposed are efficient to make micromirrors tolerate more incident optical power. The minimum optical power resulting in damage increased from 58.5 mW for the micromirror in Fig. 2 to 72.5 mW if the segmented gold slices are coated on the flexures, and to 91 mW if two flexures are designed along each side. Poly2 should be used to construct flexures if gold layer is coated on the flexures because gold layer cannot be coated directly on the top of Poly1 layer in MUMPs. The minimum optical power increased to 109.1 mW if these two methods are combined together. Compared with the micromirror of Design 1, more than 10-time increment of minimum optical power is obtained.

VI. Conclusion

Finite element models of MEMS-based micromirrors in thermal equilibrium and under continuous optical illumination have been developed, validated and used to improve the design of micromirrors for better heat transfer. Two methods are proposed and validated by optical power testing as efficient ways to increase micromirror performance for high-energy applications under the low surrounding gas pressure.

References

[1] M. Burns and V. M. Bright, "Development of microelectromechanical variable blaze gratings," *Sensors Actuators*, vol. A64, no. 11, pp. 6–14, 1998.

[2] R. A. Miller, G. W. Burr, Y. Tai, and D. Psaltis, "Electromagnetic MEMS scanning mirrors for holographic data storage," in *Proc. Solid-State Sensor Actuator Workshop*, Hilton Head Island, SC, 1996, pp. 183–186.

[3] V. P. Jaecklin, C. Linder, J. Brugger, N. F. de Rooij, J.-M. Moret, and R. Vuilleumier, "Mechanical and optical properties of surface micromachined torsional mirrors in silicon, polysilicon and aluminum," *Sensors Actuators*, vol. A43, pp. 269–275, 1994.

[4] J. D. Grimmett, "Thermal analysis of a light-reflecting digital micromirror device," in *Proc. ISPS'97*, 1997, pp. 242–247.

[5] D. M. Burns and V. M. Bright, "Optical power induced damage to microelectromechanical mirrors," *Sensors Actuators*, vol. A70, pp. 6–14, 1998.

[6] ——, "Investigation of the maximum optical power rating for a microelectromechanical device," in *Dig. Tech. Papers, 1997 Int. Conf. Solid-State Sensors Actuators Transducers '97*, vol. 1, Chicago, IL, June 16–19, 1997, pp. 335–338.

[7] J. Zhang, V. M. Bright, and Y. C. Lee, "Thermal interaction between laser and micro-mirrors," in *Spatial Light Modulators and Integrated Optoelectronic Arrays (Optical Society of America)*. Snowmass, CO: Optical Society of America, 1999, pp. 111–113.

[8] D. Koester, R. Majedevan, A. Shishkoff, and K. Marcus, *Multi-User MEMS Processes (MUMP's) Introduction and Design Rules, Rev.4*. Research Triangle Park, NC: MCNC MEMS Technology Applications Center, 1996.

[9] S. M. Sze, *Semiconductor Sensors*. New York: Wiley, 1994.

[10] R. Siegel and J. R. Howell, *Thermal Radiation Heat Transfer*, 2nd ed. New York: McGraw-Hill, 1981.

[11] F. Volklein and H. Baltes, "A microstructure for measurement of thermal conductivity of polysilicon thin films," *J. Microelectromech. Syst.*, vol. 1, no. 4, 1992.

[12] A. Bejan, *Heat Transfer*. New York: John Wiley & Sons, Inc., 1993.

[13] *IEEE Micro Electro Mechanical Systems Workshop*, Orlando, FL, Feb 1993.

Jianglong Zhang received the B.S. degree in engineering mechanics from Tsinghua University, Beijing, China, in 1998 and the M.S. degree and Ph.D. degree in mechanical engineering from the University of Colorado, Boulder, in 2000 and 2002, respectively.

He is a Modeling Engineer at Reflectivity, Inc., Sunnyvale, CA. His research interests include design and modeling of micro electro mechanical systems (MEMS) for optical applications such as display, fiber optic switch, free space optical interconnection, active alignment, and MEMS controllable microlens array. He is also working on thermal assembled position fixing, and MEMS packaging.

Yung-Cheng Lee is a Professor of mechanical engineering and a faculty member of the NSF Center for Advanced Manufacturing and Packaging of Microwave, Optical and Digital Electronics (CAMP-mode), University of Colorado, Boulder. Prior to joining the University in 1989, he was a Member of Technical Staff at AT&T Bell Laboratories, Murray Hill, NJ. He edited *Optoelectronic Packaging* (New York: Wiley, 1997) and *Manufacturing Challenges in Electronic Packaging* (New York: Chapman & Hall, 1997). His research activities include low-cost prototyping and thermal management of multichip modules, 3-D packaging, self-aligning soldering, fluxless or solderless flip-chip connections, optoelectronics packaging, process control using fuzzy-logic models, microelectromechanical systems and protein integration for microsystems.

Dr. Lee received the Presidential Young Investigator Award from the National Science Foundation, in 1990 and the Outstanding Young Manufacturing Engineer Award from SME in 1992. He was the General Chair of ASME InterPACK'01. He is the Associate Editor of the *ASME Journal of Electronic Packaging* and a Guest Editor for the IEEE Transactions on Advanced Packaging: Special Issue on MEMS/NEMS Packaging.

Adisorn Tuantranont received the B.S. degree in electrical engineering from King Mongkut's Institute of Technology, Ladkrabang, in 1995 and the M.S. and Ph.D. degrees in electrical engineering from the University of Colorado, Boulder, in 2001.

Since 2001, he has been the head of MEMS Lab, Electro-Optics Section (EOL), National Electronic and Computer Technology Center (NECTEC), Thailand. He is a Committee member withe the National Nanotechnology Center (Nanotec) (the first nanotechnology center in Thailand, under Ministry of Sciences and Technology). His research interests are in the area of micro-electro-mechanical systems (MEMS), optical communication, laser physics, microfabrication, electro-optics, optoelectronics packaging, and nanoelectronics. He has authored more than 20 international papers and journals including three patents holding.

Victor M. Bright (M'92) received the B.S.E.E. degree from the University of Colorado, Denver, in 1986, and the M.S. and Ph.D. degrees from the Georgia Institute of Technology, Atlanta, in 1989 and 1992, respectively.

He is a Professor of mechanical engineering at the University of Colorado, Boulder, and an Associate Director of the NSF Center for Advanced Manufacturing and Packaging of Microwave, Optical and Digital Electronics (CAMPmode). Prior to joining the University, he was an Associate Professor in the Department of Electrical and Computer Engineering, Air Force Institute of Technology, Wright-Patterson Air Force Base, OH, from 1992 to 1997. Dr. Bright is an author of over 50 refereed journal articles in the field of MEMS. His research activities include micro-electro-mechanical systems (MEMS), silicon micromachining, microsensors/ microactuators, opto-electronics, ceramic MEMS, MEMS reliability, and MEMS packaging. His teaching activities include manufacturing of MEMS, sensor/actuator design, and microsystem integration and packaging.

Dr. Bright received the Best Paper of Session Award from The 35th International Symposium on Microelectronics (IMAPS 2002), the Best PaperAward from the International Conference and Exhibition on Multichip Modules and High Density Packaging in 1998, the Best Paper of Session Award from the International Conference and Exhibition on Multichip Modules and High Density Packaging, in 1998, and the R.F. Bunshah Best Paper Award from the International Conference on Metallurgical Coatings and Thin Films in 1996. He serves on the Executive Committee of American Society of Mechanical Engineers (ASME) MEMS Sub-Division. He served on the Technical Program Committee for the IEEE MEMS 2000, 2001, 2002, and 2003 conferences. He also served on the Technical Program Committee for the Transducers'03.